PHYSICAL REVIEW B **85**, 081302(R) (2012)

Nonadiabatic switching of a photonic band structure: Ultrastrong light-matter coupling and slow-down of light

M. Porer,[1,2] J.-M. Ménard,[1,2,*] A. Leitenstorfer,[1] and R. Huber[1,2,†]
[1]*Department of Physics, University of Konstanz, D-78457 Konstanz, Germany*
[2]*Department of Physics, University of Regensburg, D-93040 Regensburg, Germany*

R. Degl'Innocenti,[3] S. Zanotto,[3] G. Biasiol,[4] L. Sorba,[3] and A. Tredicucci[3]
[3]*NEST, Istituto Nanoscienze-CNR and Scuola Normale Superiore, I-56127 Pisa, Italy*
[4]*Laboratorio TASC, CNR-IOM, Area Science Park, I-34149 Trieste, Italy*
(Received 13 January 2012; published 3 February 2012)

We map out the band structure of a one-dimensional photonic crystal while a 12-fs control pulse activates ultrastrong interaction with quantized electronic transitions in semiconductor quantum wells. Phase-locked multi-terahertz transients trace the buildup of a large vacuum Rabi splitting and an unexpected asymmetric formation of the upper and lower polariton bands. The pronounced flattening of the photonic bands causes a slow-down of the group velocity by one order of magnitude on the time scale of the oscillation period of light.

DOI: 10.1103/PhysRevB.85.081302 PACS number(s): 78.67.De, 42.50.Ct, 71.36.+c, 78.47.J−

In photonic crystals (PCs), periodic modulations of the refractive index have been tailored to shape photonic band structures and mold the flow of light.[1] Nonresonant light-matter interaction has been sufficient to confine optical modes with subwavelength precision[2] or to slow down the group velocity of radiation.[3,4] Particularly dramatic effects on the optical eigenmodes occur when quantized emitters are resonantly coupled to the vacuum field of a microcavity. The interaction strength is quantified by the vacuum Rabi frequency Ω_R, the rate at which a virtual photon is absorbed and spontaneously reemitted. If Ω_R exceeds cavity radiative loss and emitter dephasing, the system enters the regime of strong coupling. The eigenstates are then given by light-matter mixed modes, called cavity polaritons.[5–9]

One of the most intriguing aspects is the limit of ultrastrong coupling (USC), where Ω_R becomes comparable with the transition frequency ω_{12} of the quantum emitter itself. This extreme case has been reached by hybridizing discrete transitions between electronic subbands in semiconductor quantum wells (QWs) with the mid-infrared (MIR) photon mode of a planar waveguide.[10–12] Giant splitting of the two polariton branches, by as much as $2\Omega_R = 0.5\omega_{12}$, has been achieved in plasmonic metal structures.[13–16] A theoretical description of USC has to go beyond the rotating wave approximation.[17] The resulting squeezed quantum vacuum is expected to give rise to a variety of novel quantum electrodynamical effects.[17–19] In particular, ultrafast modulations of Ω_R have been predicted to trigger the emission of vacuum photons in a process reminiscent of the dynamical Casimir effect.[17,20] Nonadiabatic dynamics of polaritons entering the USC regime has become accessible, recently, with the aid of phase-sensitive multi-terahertz optoelectronics.[21] The planar waveguide structure explored so far, however, allowed only for limited control of the spatial dispersion of the photon field.

Here we merge the concept of a PC with nonadiabatic and ultrastrong light-matter coupling to approach full spatial and temporal control of a photonic band structure with subcycle and subwavelength precision. To this end, we combine a one-dimensional surface plasmon PC, operated in straightforward transmission, with optically switchable intersubband (ISB) resonances of semiconductor QWs. Phase-stable multi-terahertz pulses map out ultrafast snapshots of the photonic dispersion while light-matter interaction is activated by a few-femtosecond control pulse. These time-resolved measurements trace the nonadiabatic transition of the band structure from its unperturbed state to the USC regime. The dynamics is characterized by an opening of a pronounced anticrossing, a dramatic flattening of the photonic bands, and a 13-fold slow-down of the group velocity. While at late delay times the measured band structure is well reproduced by a finite-difference frequency domain (FDFD) simulation,[22] the system exhibits an intriguing asymmetry of the ultrafast build-up dynamics of the lower and upper polariton branches, suggesting a novel class of nonadiabatic quantum interference.

Figure 1(a) illustrates the design of our device. A 2-μm-thick $Al_{0.95}Ga_{0.05}As$ cladding layer, followed by a sequence of 50 pairs of undoped GaAs QWs and $Al_{0.33}Ga_{0.67}As$ barriers, are grown epitaxially on undoped GaAs (thickness: 350 μm). The width of 8.3 nm of each QW is chosen such that the energetic distance between the lowest electronic conduction subbands amounts to 120 meV (29 THz). A gold grating with a period of $a = 3.6$ or 4.1 μm is thermally evaporated on top of the heterostructure to shape the optical modes inside the QW region. The device may be considered as a one-dimensional metallic PC, which folds the modes guided by the cladding layer and the MQW into the first Brillouin zone.[15] In contrast to Ref. 21, the full dispersion of the eigenmodes is mapped out by recording the transmission of ultrabroadband multi-terahertz pulses [Fig. 1(b)]. Electro-optic sampling traces the oscillating probe field directly in the time domain. Figure 1(c) depicts a typical wave form incident on the device. Within its FWHM, the pulse encompasses only three optical cycles, centered at a frequency of 29 THz [Fig. 1(d)]. Comparing the Fourier transforms of incident and transmitted transients allows us to retrieve the transmission spectra. Eigenmodes are identified via the spectral position of local transmission maxima [Fig. 1(e)]. The full band structure of all supported electromagnetic modes is resolved as a function of the in-plane

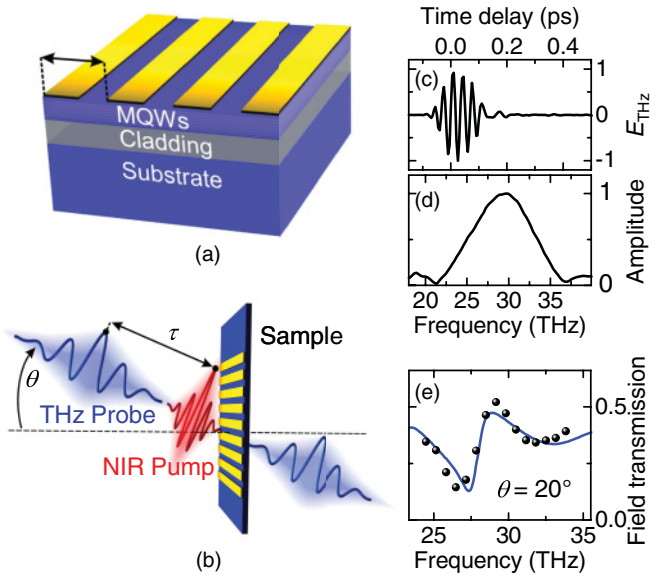

FIG. 1. (Color online) (a) Sample design: heterostructure consisting of 50 repetitions of 8.3-nm-thick GaAs QWs separated by 30-nm-thick $Al_{0.33}Ga_{0.67}As$ barriers grown on top of a 2-μm-thick $Al_{0.95}Ga_{0.05}As$ cladding layer and an undoped GaAs substrate. The planar waveguide defined by the refractive index contrast ($n_{air} = 1$, $n_{MQW} = 3.2$, $n_{cladd} = 2.8$) is structured as a PC via a lateral gold grating. (b) Transmission of multi-terahertz pulses maps out the band structure of the system. A co-propagating NIR pump pulse injects electrons in the MQWs (delay time: τ), activating ultrastrong light-matter coupling. (c) Electro-optically sampled multi-terahertz field transient and (d) corresponding amplitude spectrum. (e) Measured (dots) and calculated (line) field transmission of the equilibrium PC structure ($a = 4.1\,\mu$m) at $\theta = 20^\circ$.

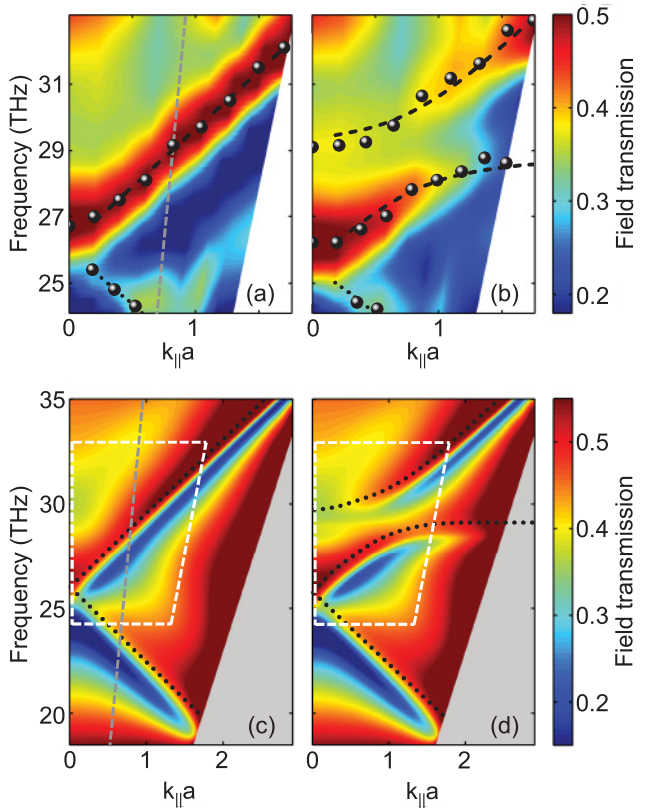

FIG. 2. (Color online) Transmission spectra of the PC structure ($a = 4.1\,\mu$m) as a function of $k_{||}$. Experimental results in (a) equilibrium and (b) 1000 ps after photo-activation of the ISB transition ($\Phi = 1.6\,mJ/cm^2$) for $0 \leqslant \theta \leqslant 40^\circ$. Black spheres: experimental position of local transmission peaks indicate the eigenmodes. Dashed black lines: numerically adapted polariton dispersion. (c) and (d) FDFD simulations of the unpumped and pumped sample, respectively, for $0 \leqslant \theta \leqslant 89.9^\circ$. Black dotted curves indicate the eigenmodes in all panels. Dashed grey lines in (a) and (c): cross sections displayed in Fig. 1(e). White tetragons in (c) and (d): area covered by the experiments in (a) and (b).

momentum $k_{||}$ by varying the angle of incidence θ of the p-polarized probe beam. A copropagating near-infrared (NIR) pump pulse centered at 1.55 eV ($\lambda_c = 800$ nm) injects electrons into the lowest electronic subband $|1\rangle$, activating an ISB transition. P-polarized optical modes may strongly couple to this resonance. The duration $t_p = 12$ fs of the control pulse is kept distinctly shorter than the oscillation period of the MIR light in order to facilitate nonadiabatic control of the band structure. The subsequent ultrafast dynamics is resolved by varying the time delay (τ) between control and probe pulses.

Figure 2 shows typical MIR transmission spectra as a function of $k_{||}$. In the unpumped device [Fig. 2(a)], we identify two photonic bands in the frequency window between 24 and 32 THz. Both modes are degenerate at $\omega/2\pi = 26.6$ THz, in the center of the Brillouin zone, but split with increasing $k_{||}$. Qualitatively these states arise from guided light which is Bragg scattered by the reciprocal lattice vectors π/a and $-\pi/a$, respectively. Photo-injecting electrons into the lowest electronic subband $|1\rangle$ of each QW, with a NIR pump fluence of $\Phi = 1.6\,mJ/cm^2$, induces a strong modification of the band dispersion, as directly mapped out in Fig. 2(b). This snapshot of the band structure was taken at a delay time $\tau = 1$ ns after the arrival of the pump pulse. The interaction between the ISB resonance and the upper photon band causes a marked energy gap between a lower and an upper polariton branch [Fig. 2(b), black spheres], at $\tau = 1$ ns. The minimum separation of 3 THz of the two eigenmodes occurs at $\theta = 20^\circ$ and may be directly identified with the Rabi splitting $2\Omega_R/2\pi$. Notably both polariton bands are strongly flattened as compared to the unperturbed photon dispersion.

To gain further insight into the microscopic nature of the eigenmodes, we model these transmission maps with an FDFD calculation [Figs. 2(c) and 2(d)]. Quantitative agreement with the experiment is obtained only when both waveguiding by total internal reflection and surface plasmons at the metallic grating are taken into account. Our simulations even allow us to recover details such as the Fano-like lineshape of the bare photon modes [Fig. 1(e)].[23] In order to reproduce the band structure of the strongly coupled system [Fig. 2(d)], we treat the ISB transition classically via an effective refractive index[10] and achieve good agreement with the experimental transmission map of Fig. 2(b). The dispersion of all bands, the strength of light-matter coupling, and the absolute value of field transmission are adequately reproduced.

The transmission spectra depend sensitively on pump fluence Φ and delay time τ, as studied rigorously in Fig. 3. For these experiments, the substrate of the heterostructure is

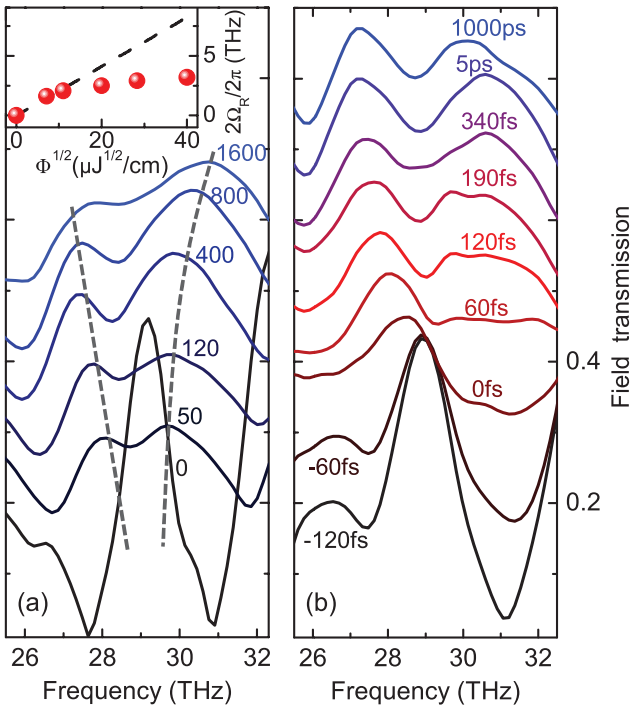

FIG. 3. (Color online) Transmission spectra of the PC structure ($a = 3.6\,\mu$m, no substrate) showing the polariton formation at the anticrossing point ($\theta = 13^\circ$). To ensure that additional membrane guided modes are far above our measurement window, we now couple the ISB transition to the lower photon band by setting a to 3.6 μm. (a) Spectra measured at $\tau = 1000$ ps for various pump fluences Φ (stated in μJ/cm^2). Inset: $2\Omega_R/2\pi$ as a function of $\Phi^{1/2}$. (b) Transmission for selected τ with $\Phi = 1600\,\mu$J/cm^2. A maximum splitting of 3.4 THz is reached at $\tau = 340$ fs. All spectra are separated by a linearly increasing offset.

locally removed by chemical etching to obtain a free-standing membrane with minimal dispersion for ultrafast laser pulses. Pump and probe beams are directed onto the rear side of the sample to inject and detect a homogeneous distribution of carriers and prevent diffusion effects from affecting the intrinsic dynamics. In contrast to the complex prism geometry and tilted pulse fronts used in earlier studies,[21] femtosecond temporal synchronization is now warranted by straightforward collinear propagation of the NIR control and the terahertz probe pulses.

Figure 3(a) shows spectra for various values of Φ, measured at a fixed delay time $\tau = 1$ ns with θ set to the anticrossing point. In the unpumped case, we observe a single maximum at 29 THz with a narrow width of 1.4 THz (FWHM) corresponding to a quality factor of $Q = 20$. With increasing fluence, the single peak splits into two polariton branches of comparable strength. Ω_R scales with the square root of the pump fluence [inset of Fig 3(a)] for $\Phi < 120\ \mu$J/cm^2, analogously to the situation in planar waveguides.[17] Yet the Rabi frequency starts to saturate at $\Phi = 400\ \mu$J/cm^2, when a pulse area of π for interband transitions is approached. We estimate the average carrier density to saturate at $N_{2D} = 3 \times 10^{11}$ cm^{-2} in our structure.

In order to explore how rapidly the hybridization of the photonic band structure with the ISB transition proceeds, we vary the delay time τ between -120 fs and 1000 ps [Fig. 3(b)]. The pump fluence is kept constant at $\Phi = 1.6$ mJ/cm^2. For negative delay times $\tau \leqslant -60$ fs, the transmission spectra are dominated by a single eigenmode at $\omega_{12}/2\pi = 29$ THz, characteristic of the unpumped state. When the maxima of the pump and probe pulses coincide at $\tau = 0$, an abrupt qualitative change of the transmission spectrum manifests itself. Instead of the bare eigenmode, two resonances occur: a strong peak centered at $\omega_L/2\pi = 28.2$ THz and a weaker one at $\omega_U/2\pi = 30.5$ THz, corresponding to the lower and upper polariton branch, respectively. Intriguingly, the upper branch exhibits a lower amplitude than the lower branch, it also remains spectrally much broader and even splits into two maxima during the initial time window $0 \leqslant \tau \leqslant 340$ fs. At $\tau = 340$ fs, a maximum splitting of $2\Omega_R/2\pi = 3.4$ THz is reached, which amounts to 12% of $\omega_{12}/2\pi$, exceeding even values demonstrated with static doping.[15] At this point, both polariton branches are comparable in intensity and width. Between $\tau = 5$ and 1000 ps, the vacuum Rabi frequency shrinks slightly by 10% due to carrier recombination.

The surprising and consistenly reproducible asymmetric buildup of the polaritons is in stark contrast to the dynamics seen in planar waveguides.[21] Since the only difference of the design is given by the photonic band structure, this qualitative discrepancy clearly indicates that the peculiar band structure of the PC sets a characteristic switch-on time for the formation of USC. Due to energy-time uncertainty, abrupt switching events have to involve a broad spectrum of eigenmodes. Contrary to planar waveguides, this spectrum is strongly structured in the case of a PC. The simultaneous coherent interaction of ISB transitions with higher photonic bands may thus lead to discrete quantum interference during the activation of USC. In the current situation, we tentatively suggest that nonadiabatic mixing of the upper polariton branch with the next higher photonic band may play a dominant role. A quantitative model of this fascinating new class of ultrafast quantum phenomena is yet missing. Our observations call for a universal theory treating nonadiabatic quantum electrodynamics and quantum kinetic carrier dynamics, on equal footing.

Under the action of extremely strong light-matter coupling, the slope of polaritonic bands in Fig. 2(b) is profoundly reduced. This effect gives rise to a slow-down of the group velocity $d\omega/dk_{||}$ of light inside the QW region. As a

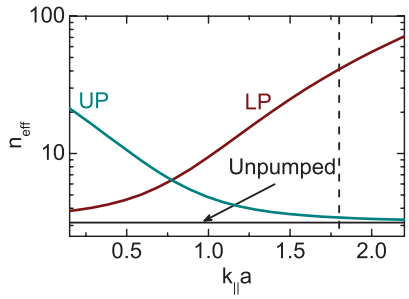

FIG. 4. (Color online) n_{eff} at the spectral peak position of the upper photonic modes in the pumped and unpumped sample, as represented by the black curves in Figs. 2(a) and 2(b). The solid curve is the theoretical $n_{\text{eff}} = 3.15$ of the light mode propagating inside the unpumped QW region.

quantitative measure, we extract the effective group index of refraction n_{eff} as a function of $k_{||}$ (Fig. 4) from a numerically adapted polariton dispersion curve[24] on the experimental band structure [Fig. 2(e)], without resorting to a rotating wave approximation. While n_{eff} reflects the theoretical value of 3.15 in the unpumped sample, the extracted n_{eff} increases for the lower polariton branch to 41 at the highest $k_{||}$ values covered in our experiment. Coherent photon population, which is initially prepared in the bare grating waveguide by the multi-terahertz transients, is thus abruptly transferred into a polaritonic band, decreasing its group velocity by a factor of 13.

Slow light reaching speeds down to only few tens of meters per second has been observed with diverse experimental methods.[25–27] However most of the previous techniques suffer from a limited bandwidth that hinders their practical applications. In this context, the present experimental scheme holds great potential because of its ability to slow down light over a bandwidth corresponding to a significant fraction of the carrier frequency. In this regards, our results compare advantageously with state-of-the-art broadband generation of slow light in PCs.[3,4] The demonstrated control of the band stucture may ultimately allow a broadband storage of light by transferring a photon population from a leaky equilibrium photo-plasmonic band to a nonleaky LP branch below the light line. Most importantly, our scheme is faster by multiple orders of magnitude than previous approaches toward manipulation of slow light. Hence it provides the possibility of investigating ultrafast switching of the slow-light regime.

In conclusion, we demonstrate a nonadiabatic activation of extremely strong plasmon-assisted light-matter interaction in a photonic crystal. Electro-optic sampling of the amplitude and phase-sensitive response of the device allows us to map out the full band structure with a time resolution better than a single oscillation cycle of light. On the femtosecond scale the band structure is dramatically changed, featuring an opening of a large Rabi splitting of $2\Omega_R/2\pi = 3.4$ THz and a flattening of the photonic bands. Our approach opens the door toward complete band structure engineering in all four dimensions. A completely new area of ultrafast quantum electrodynamical phenomena involving the abrupt creation of white and black hole horizons via slow light as well as vacuum photon emission may come into reach.[28]

Fruitful discussions with C. Ciuti and S. De Liberato are gratefully acknowledged. This work was supported by Deutsche Forschungsgemeinschaft (DFG) via Emmy Noether grant HU-1598 and the Alexander von Humboldt Foundation.

*jean-michel.menard@ur.de

†rupert.huber@ur.de;

[1] J. D. Joannopoulos, S. G. Johnson, J. N. Winn, and R. D. Meade, *Photonic Crystals: Molding the Flow of Light* (Princeton University Press, Princeton, New Jersey, 2008).

[2] J. S. Foresi, P. R. Villeneuve, J. Ferrera, E. R. Thoen, G. Steinmeyer, S. Fan, J. D. Joannopoulos, L. C. Kimerling, H. I. Smith, and E. P. Ippen, Nature (London) **390**, 143 (1997).

[3] M. D. Settle, R. J. P. Engelen, M. Salib, A. Michaeli, L. Kuipers, and T. F. Krauss, Opt. Express **15**, 219 (2007).

[4] Y. A. Vlasov, M. O'Boyle, H. F. Hamann, and S. J. McNab, Nature (London) **438**, 65 (2005).

[5] C. Weisbuch, M. Nishioka, A. Ishikawa, and Y. Arakawa, Phys. Rev. Lett. **69**, 3314 (1992).

[6] A. Imamoglu, R. J. Ram, S. Pau, and Y. Yamamoto, Phys. Rev. A **53**, 4250 (1996).

[7] J. Kasprzak, M. Richard, S. Kundermann, A. Baas, P. Jeambrun, J. M. J. Keeling, F. M. Marchetti, M. H. Szymanska, R. André, J. L. Staehli, V. Savona, P. B. Littlewood, B. Deveaud, and Le Si Dang, Nature (London) **443**, 409 (2006).

[8] H. Deng, G. Weihs, C. Santori, J. Bloch, and Y. Yamamoto, Science **298**, 199 (2002).

[9] A. Delteil, A. Vasanelli, P. Jouy, D. Barate, J. C. Moreno, R. Teissier, A. N. Baranov, and C. Sirtori, Phys. Rev. B **83**, 081404(R) (2011).

[10] D. Dini, R. Köhler, A. Tredicucci, G. Biasiol, and L. Sorba, Phys. Rev. Lett. **90**, 116401 (2003).

[11] E. Dupont, J. A. Gupta, and H. C. Liu, Phys. Rev. B **75**, 205325 (2007).

[12] A. A. Anappara, S. De Liberato, A. Tredicucci, C. Ciuti, G. Biasiol, L. Sorba, and F. Beltram, Phys. Rev. B **79**, 201303 (2009).

[13] Y. Todorov, A. M. Andrews, I. Sagnes, R. Colombelli, P. Klang, G. Strasser, and C. Sirtori, Phys. Rev. Lett. **102**, 186402 (2009).

[14] Y. Todorov, A. M. Andrews, R. Colombelli, S. De Liberato, C. Ciuti, P. Klang, G. Strasser, and C. Sirtori, Phys. Rev. Lett. **105**, 196402 (2010).

[15] S. Zanotto, G. Biasiol, R. Degl'Innocenti, L. Sorba, and A. Tredicucci, Appl. Phys. Lett. **97**, 231123 (2010).

[16] M. Geiser, C. Walther, G. Scalari, M. Beck, M. Fischer, L. Nevou, and J. Faist, Appl. Phys. Lett. **97**, 191107 (2010).

[17] C. Ciuti, G. Bastard, and I. Carusotto, Phys. Rev. B **72**, 115303 (2005).

[18] E. Yablonovitch, Phys. Rev. Lett. **62**, 1742 (1989).

[19] C. M. Wilson, G. Johansson, A. Pourkabirian, M. Simoen, J. R. Johansson, T. Duty, F. Nori, and P. Delsing, Nature (London) **479**, 376 (2011).

[20] S. De Liberato, C. Ciuti, and I. Carusotto, Phys. Rev. Lett. **98**, 103602 (2007).

[21] G. Günter, A. A. Anappara, J. Hees, A. Sell, G. Biasiol, L. Sorba, S. De Liberato, C. Ciuti, A. Tredicucci, A. Leitenstorfer, and R. Huber, Nature (London) **458**, 178 (2009).

[22] R. C. Rumpf, A. Tal, and S. M. Kuebler, J. Opt. Soc. Am. A **24**, 3123 (2007).

[23] S. Zanotto, R. Degl'Innocenti, L. Sorba, A. Tredicucci, and G. Biasiol, Phys. Rev. B **85**, 035307 (2012).

[24] J. J. Hopfield, Phys. Rev. **112**, 1555 (1958).

[25] M. S. Bigelow, N. N. Lepeshkin, and R. W. Boyd, Science **301**, 200 (2003).

[26] P.-C. Ku, F. Sedgwick, C. J. Chang-Hasnain, P. Palinginis, T. Li, H. Wang, S.-W. Chang, and S.-L. Chuang, Opt. Lett. **29**, 2291 (2004).

[27] A. V. Turukhin, V. S. Sudarshanam, M. S. Shahriar, J. A. Musser, B. S. Ham, and P. R. Hemmer, Phys. Rev. Lett. **88**, 023602 (2001).

[28] F. Belgiorno, S. L. Cacciatori, M. Clerici, V. Gorini, G. Ortenzi, L. Rizzi, E. Rubino, V. G. Sala, and D. Faccio, Phys. Rev. Lett. **105**, 203901 (2010).